where $\mathbb{E}[O_i^2] = (\log(q_{0,0}/q_{1,0}))^2 \Pr[s_i = 0] + (\log(q_{0,1}/q_{1,1}))^2 \Pr[s_i = 1]$. Finally, the variance value of L_t is given as follows:

$$\mathbb{V}\mathrm{ar}\left[\sum_{i=1}^{t} a^{t-i}O_i + a^t L_0 + b\left(\frac{1-a^t}{1-a}\right)\right] = \mathbb{V}\mathrm{ar}[O_i]\sum_{i=1}^{t} a^{2(t-i)} = \mathbb{V}\mathrm{ar}[O_i]\left(\frac{1-a^{2t}}{1-a^2}\right). \quad (28)$$

REFERENCES

[1] N. Devroye, M. Vu, and V. Tarokh, "Cognitive radio networks: Highlights of information theoretic limits, models and design," *IEEE Signal Process. Mag.*, vol. 25, no. 6, pp. 12–23, Nov. 2008.

[2] F. F. Digham, M.-S. Alouini, and M. K. Simon, "On the energy detection of unknown signals over fading channels," in *Proc. ICC*, Anchorage, AK, May 2003, pp. 3575–3579.

[3] T. Yücek and H. Arslan, "A survey of spectrum sensing algorithms for cognitive radio applications," *IEEE Commun. Surveys Tuts.*, vol. 11, no. 1, pp. 116–130, First Quarter, 2009.

[4] A. Ghasemi and E. S. Sousa, "Opportunistic spectrum access in fading channels through collaborative sensing," *J. Commun.*, vol. 2, no. 2, pp. 71–82, Mar. 2007.

[5] A. Ghasemi and E. S. Sousa, "Asymptotic performance of collaborative spectrum sensing under correlated log-normal shadowing," *IEEE Commun. Lett.*, vol. 11, no. 1, pp. 34–36, Jan. 2007.

[6] T. Kailath and H. V. Poor, "Detection of stochastic processes," *IEEE Trans. Inf. Theory*, vol. 44, no. 6, pp. 2230–2231, Oct. 1998.

[7] Y. Sung, L. Tong, and H. V. Poor, "Neyman-pearson detection of gauss-Markov signals in noise: Closed-form error exponent and properties," *IEEE Trans. Inf. Theory*, vol. 52, no. 4, pp. 1354–1365, Apr. 2006.

[8] Y. Chen, Q. Zhao, and A. Swami, "Distributed spectrum sensing and access in cognitive radio networks with energy constraint," *IEEE Trans. Signal Process.*, vol. 57, no. 2, pp. 783–797, Feb. 2009.

[9] Q. Zhao, L. Tong, A. Swami, and Y. Chen, "Decentralized cognitive MAC for opportunistic spectrum access in Ad Hoc networks: A POMDP framework," *IEEE J. Sel. Areas Commun.*, vol. 25, no. 3, pp. 589–600, Apr. 2007.

[10] S. Geirhofer, L. Tong, and B. M. Sadler, "Dynamic spectrum access in the time domain: Modeling and exploiting white space," *IEEE Commun. Mag.*, vol. 45, no. 5, pp. 66–72, May 2007.

[11] G. Ghosh, C. Cordeiro, D. P. Agrawal, and M. B. Rao, "Markov chain existence and hidden Markov models in spectrum sensing," in *Proc. PerCom*, Galveston, TX, Mar. 2009, pp. 1–6.

[12] H. Urkowitz, "Energy detection of unknown deterministic signals," *Proc. IEEE*, vol. 55, no. 4, pp. 523–531, Apr. 1967.

[13] M. Rashid, M. Hossain, E. Hossain, and V. Bhargava, "Opportunistic spectrum scheduling for multiuser cognitive radio: A queueing analysis," *IEEE Trans. Wireless Commun.*, vol. 8, no. 10, pp. 5259–5269, Oct. 2009.

[14] J. Neyman and E. Pearson, "On the problem of the most efficient tests of statistical hypotheses," *Philosoph. Trans. Roy. Soc. London, Ser. A*, vol. 231, pp. 289–337, Jan. 1993.

[15] Q. Zhao and B. M. Sadler, "A survey of dynamic spectrum access," *IEEE Signal Process. Mag.*, vol. 24, no. 3, pp. 79–89, May 2007.

[16] *Draft Standard for Wireless Regional Area Networks Part 22: Cognitive Wireless RAN Medium Access Control (MAC) and Physical Layer (PHY) Specifications: Policies and Procedures for Operation in the TV Bands*, IEEE Std. P802.22/D0.5, Mar. 2008.

[17] R. L. Kashyap, "Identification of a transition matrix of a Markov chain from noisy measurements of state," *IEEE Trans. Inf. Theory*, vol. IT-16, no. 2, pp. 161–166, Mar. 1970.

[18] T. Ryden, "On recursive estimation for hidden Markov models," *Stoch. Process. Appl.*, vol. 66, no. 1, pp. 79–96, Feb. 1997.

[19] U. Holst and G. Lindgren, "Recursive estimation in mixture models with Markov regime," *IEEE Trans. Inf. Theory*, vol. 37, no. 6, pp. 1683–1690, Nov. 1991.

Measurements and Characterizations of Air-to-Ground Channel Over Sea Surface at C-Band With Low Airborne Altitudes

Yu Song Meng, *Member, IEEE*, and Yee Hui Lee, *Member, IEEE*

***Abstract*—This paper presents an experimental study of air-to-ground channels over sea surface at the C-band (5.7 GHz) with low airborne altitudes (0.37–1.83 km) through wideband channel measurements. In this paper, the multipath statistics and the propagation loss at different airborne altitudes are estimated and analyzed. It is observed that about 95% (86%) of the measured channel responses can be represented by the 3-ray (2-ray) multipath model. As the airborne altitude decreases, there is a higher probability for the appearance of multipath components. Moreover, it is found that the evaporation duct and elevated duct over the sea surface are the two important factors that can significantly affect the over-water air-to-ground communication link. These ducts can also decrease the rate of radio-wave attenuation, i.e., a decrease in path-loss exponent n in the log-distance path-loss models.**

***Index Terms*—Aeronautical communications, channel modeling, ducting, microwave landing system (MLS), multipath channels.**

I. INTRODUCTION

Research on wireless communication channels at C-band for air-to-ground links has become attractive in recent years due to the implementation of a C-band microwave landing system (MLS) in aviation navigation. The environment for MLS applications can mainly be classified into either the airport surface environment or the air-to-ground communication environment. Recently, Matolak *et al.* [1]–[3] contributed extensive studies on the wideband channel measurement and characterization for airport surface environments at the 5-GHz band with 20-ns delay resolution. Their investigations included both large airports [2] and small airports [3]. In addition to their works, a comparative study of the current conventional very high-frequency band and the upcoming C-band MLS was reported by Tu *et al.* [4], where an air-to-ground link over land at 5.8 GHz was investigated. In their study, the C-band air-to-ground channel over land was estimated to undergo free-space conditions when the propagation was not through foliage [5] and is not influenced by other environmental effects. A large number of works relating to the characterization and modeling of the air-to-ground channel over land areas (desert, mountain, etc.) at other frequencies ($\sim$1.5 GHz, $\sim$2.3 GHz) were also reported in [6]–[8].

From the literature, little research is done on the study of the air-to-ground channel over a sea surface at the C-band. The most recent work done in this area is on the modeling of a multipath propagation channel over sea water at 8.0 GHz [9]. In [9], results show that a 3-ray multipath model consisting of a line-of-sight (LoS) path and two

Manuscript received July 30, 2010; revised November 12, 2010 and February 15, 2011; accepted March 23, 2011. Date of publication April 5, 2011; date of current version May 16, 2011. This work was supported in part by the Defence Science and Technology Agency, Singapore. The review of this paper was coordinated by Prof. C. P. Oestges.

Y. S. Meng was with the School of Electrical and Electronic Engineering, Nanyang Technological University, Singapore 639798. He is now with the RF and Optical Department, Institute for Infocomm Research, Singapore 138632 (e-mail: ysmeng@ieee.org, meng0006@ntu.edu.sg).

Y. H. Lee is with the School of Electrical and Electronic Engineering, Nanyang Technological University, Singapore 639798 (e-mail: eyhlee@ntu.edu.sg).

Color versions of one or more of the figures in this paper are available online at http://ieeexplore.ieee.org.

Digital Object Identifier 10.1109/TVT.2011.2136364

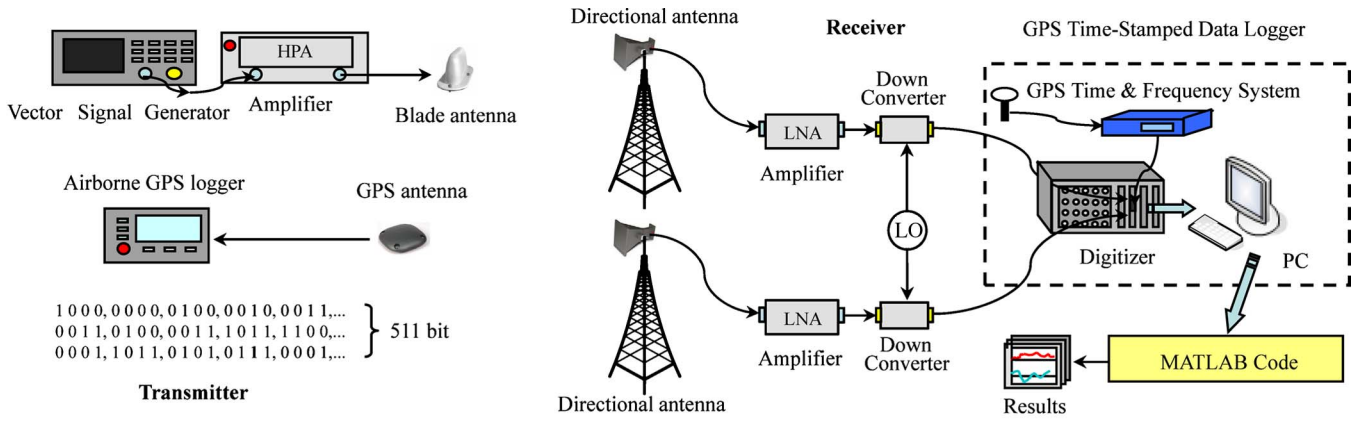

(a)

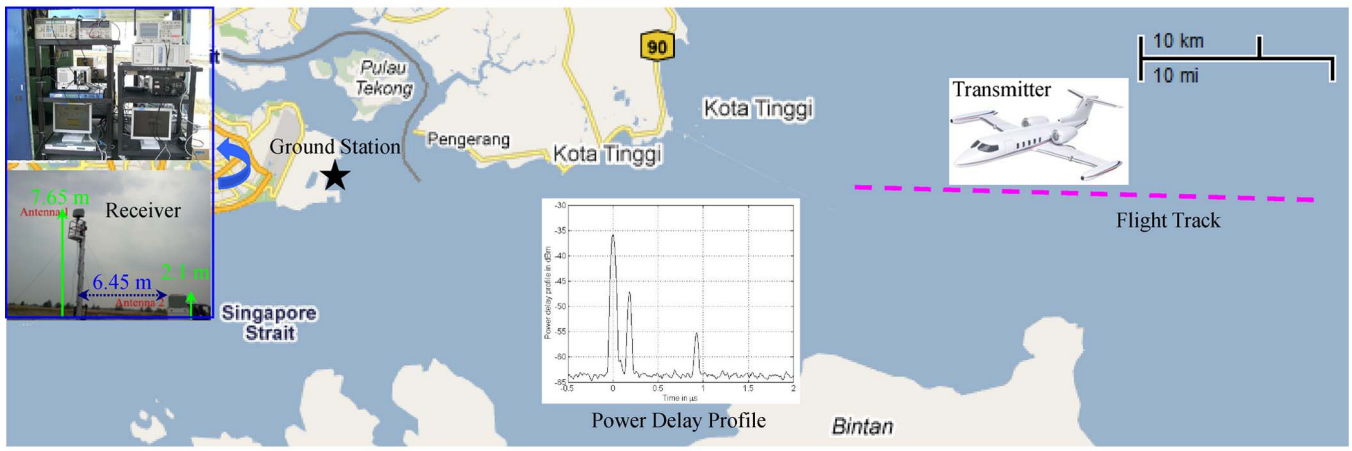

(b)

Fig. 1. Wideband channel measurement setup and locations. (a) Channel sounding and data logging techniques. (b) Measurement site and flight tracks. ($\star$) Location of ground station. (Dash-dotted) Flight tracks.

reflected propagation paths provides a good fit to the measured channel responses. However, the path-loss modeling of an air-to-ground link over the sea surface is less investigated. Propagation over sea surface is well recognized to be affected by ducting layers. For example, an evaporation duct above the sea surface can result in a substantial increase in the received signal strength at frequencies above 3 GHz [10]. Therefore, it is of great interest to study the effects of such ducts in the characterization and modeling of air-to-ground channels over a sea surface at the C-band. The results are important for modern military and commercial applications in seashore countries.

In our previous works [11], [12], channel characterization and modeling at the C-band (5.7 GHz) for a small seashore airport surface environment has been reported [11]. When compared with the channel information reported in [1] and [2], similar results for the path-loss exponent n are obtained but with a smaller shadowing value in this airport (about 4.1 dB) due to less-crowded air traffic. Moreover, air-to-ground channels over sea surfaces at high airborne altitudes (6.1–12.2 km) have been investigated in [12] with both narrowband and wideband measurements. It was found that the transmitted signal can be obstructed (shadowed) by the aircraft's body during a predefined turning maneuvering when the antenna is mounted on top of an aircraft for air-to-ground communication.

As a continued work, the main objective of this paper is to perform a detailed study of the air-to-ground channel over the sea surface at the C-band with low airborne altitudes to investigate the effects from the sea-surface reflections and the possible influence from evaporation duct/elevated duct. In Section II, the channel sounding technique is described, together with a brief description of the measurement setup and the measurement procedures. In Section III, multipath channel statistics with low airborne altitudes are estimated and compared with the reported multipath information for similar propagation scenarios. This is followed by the characterization and modeling of the radio-wave propagation loss over the sea surface with low airborne altitudes in Section IV. Finally, Section V gives a summary of the analyses performed in this paper.

II. Measurement Campaign

A. Channel Sounding Technique and Measurement Setup

The spread-spectrum technique *maximal-length pseudonoise (PN) sequence* was implemented for channel sounding at the transmitter as in [1]–[3] and [7]. In our measurements, a 511-bit PN sequence was transmitted at a rate of 20 Mchip/s and modulated using binary phase-shift keying. This allows for a time resolution of 50 ns for the measurements [13]. As shown in Fig. 1(a), the predefined signal was transmitted by a vector signal generator and then passed through a high-power amplifier, before being radiated into the channel of interest via a vertically polarized omnidirectional blade antenna. This blade antenna was mounted on the head of an aircraft (Learjet 35A in this study) with an effective radiated power of 40 dBm. During the flight, Global Positioning System (GPS) data were continuously logged through a GPS receiver installed on the aircraft throughout the measurements to obtain the instantaneous altitude, longitude, latitude, pitch, roll, and yaw coordinates of the moving aircraft.

TABLE I
PROBABILITY FOR THE OCCURRENCE OF MULTIPATH DURING FLIGHT

Altitude	Channel	1-ray	2-ray	3-ray	4-ray	5-ray	6-ray	7-ray
1.83 km	1	56.1%	38.2%	5.7%				
	2	89.5%	10%	0.5%				
0.91 km	1	75.9%	20.8%	2.98%	0.32%			
	2	85.1%	14.4%	0 %	0.5%			
0.37 km	1	62.4%	23.5%	8.5%	3.34%	1.67%	0.42%	0.17%
	2	75.6%	17.7%	4.74%	1.11%	0.7%	0 %	0.15%

*Channel 1 is with an antenna height of 7.65 m, and Channel 2 is with an antenna height of 2.10 m

At the receiver, two identical directional antennas with a beam width of 20° in azimuth and 25° in elevation were used to create a height (5.55 m) and space (6.45 m) diversity receptor, as shown in Fig. 1. The received signal was amplified and down-converted to a 22-MHz intermediate-frequency signal and sampled at a rate of 100 Msample/s. The total gain of each receiver front end consisting of an antenna, a low-noise amplifier, a mixer, and a low-pass filter is about 80 dB. All the data recorded were stamped with the GPS time to synchronize the measured data with the aircraft location. A detailed description of the channel sounder that was used in the measurement campaign can be found in [13].

B. Measurement Procedures

Wideband air-to-ground channel measurements with low airborne altitudes were conducted over the South China Sea at 5.7 GHz in February 2009. The coastal area on the eastern side of Singapore ($1°20'07''\text{N}, 104°01'16''\text{E}$), as shown in Fig. 1(b), was selected as the ground station. With the flight path shown in Fig. 1(b), the radio wave mainly propagated over the sea surface, and there was no blockage of the signal. In this paper, the radio-wave propagation along the flight paths, as illustrated in Fig. 1(b), was investigated with the airborne altitudes of 0.37, 0.91, and 1.83 km, respectively. The flight paths were straight toward the ground station, and therefore, the shadowing effect by the aircraft maneuvering [12], [14] can be minimized and kept almost constant. During the measurements, the weather was initially sunny, followed by a cloudy weather condition. However, no rainfall was experienced throughout the flight trial.

III. ANALYSIS OF THE MULTIPATH CHANNEL

The air-to-ground propagation channel can be modeled as a linear time-variant system, whose complex baseband equivalent channel impulse response $h(t,\tau)$ can be expressed as

$$h(t,\tau) = \sum_{k=0}^{N} a_k(t) \exp\{j\varphi_k(t)\}\, \delta\{\tau - \tau_k(t)\} \tag{1}$$

where t and τ are the observation and application times of the impulse, respectively; a_k, τ_k, and φ_k are the time-varying amplitude, propagation delay, and phase shift of the kth multipath component, respectively; and N is the number of multipath components of the channel of interest.

In this paper, the empirical channel impulse response $h(t,\tau)$ of the air-to-ground channel at 5.7 GHz was obtained by correlating the known transmitted signal with the received signal [13], [15]. More than 100 000 channel impulse responses were obtained and processed for each flight profile (0.37, 0.97, and 1.83 km), over a 2-h (afternoon) flight trial. An example of the instantaneous power delay profile (PDP), which is proportional to $|h(t,\tau)|^2$, is shown in Fig. 1(b). The multipath information for each flight profile were then estimated from the PDPs, as in [16], and tabulated in Table I for analysis. The number of multipath in each instantaneous PDP along the flight track shown in Fig. 1(b) is determined. If there are 6144 instantaneous PDPs with four propagating rays and there are a total of 183 808 instantaneous PDPs along the flight track, there will be about 3.34% of instantaneous PDPs with 4-rays shown in Table I. It can be seen that, as the airborne (transmitter) altitude decreases, there are more reflected rays appearing in the channel. This can be explained using the "Rayleigh criterion" [17]; a surface is considered rough only if $\sigma > \lambda/(8\cos\theta_i)$, where σ is the surface roughness, λ is the wavelength of the signal, and θ_i is the incident angle of the incoming wave. In our study, when the airborne (transmitter) altitude decreases, the incident angle θ_i increases, and thus, $\lambda/(8\cos\theta_i)$ increases. Hence, the sea surface appears to be "smoother," and thus, specular reflections become stronger. The experimental results also show that the receiver with a higher antenna height (i.e., 7.65-m antenna height for Channel 1) has a higher probability of receiving sea-surface reflected rays over a percentage of time. This could be due to the height difference between the two receivers.

The observation of multipath propagation shows the possibility of implementing a diversity system [17] at the ground station to mitigate multipath fading. For example, for the channel at a flight altitude of 0.37 km, there is a probability of about 30% for both channels to suffer a propagation loss greater than 154 dB. With selection diversity (the simplest form of diversity systems) employed at the ground station as in [16], the probability for the channel to suffer a propagation loss greater than 154 dB is reduced to about 24%. This is an improvement of about 6% in the performance of the link. However, it should be noted that space diversity at the ground station may not be helpful for overcoming the signal obstruction created by the aircraft maneuvering (the shadowing induced by the aircraft body as in [12]) during air-to-ground transmission [14].

Moreover, from Table I, it can be observed that, about 95% of the estimated air-to-ground channel responses can be represented by a 3-ray multipath model. This is similar to the observations found in [9] for the air-to-ground channel over sea water at 8.0 GHz. The researchers in [9] reported that, for an air-to-ground channel at 8 GHz over a sea surface with a flight altitude of 0.76 km, a 3-ray model consisting of the LoS path and two reflected propagation paths provides a good fit for the measured channel impulse responses. One of the reflected propagation paths is a strong specular reflection determined by the geometry defined by the airborne transmitter, the ground-based receiver, and the sea surface. However, based on our measurement results, the 3-ray propagation only exists about 8.5%, or less, of the time, and the power of the third ray is low, compared with the first and second rays. It is also found that about 86% of the measurement results can be represented by a 2-ray model taking into consideration

all the flight altitudes in this measurement campaign. It should be noted that these measurements are based on the channel sounding with a time resolution of 50 ns. Therefore, when two echoes arrive within 50 ns of each other, they will appear as one multipath in the estimated PDP.

Furthermore, delay information for the air-to-ground channel is estimated as in [21]. This could provide a clearer idea about the over-sea propagation conditions. The median root mean square (RMS) delay spreads for channels 1 and 2 are found to be 20 and 38 ns at the airborne altitude of 1.83 km, 30 and 35 ns at the airborne altitude of 0.91 km, and 335 and 480 ns at the airborne altitude of 0.37 km. The RMS delay spread reported in [9] is 31 ns for calm seas and 20 ns for rough seas with an airborne altitude of 0.76 km at 8.0 GHz. Comparing these results, it can be concluded that similar propagation occurs at the airborne altitudes of 0.76 km [9], 0.91 km, and 1.83 km (this study). However, as the airborne altitude decreases to 0.37 km, as presented in this study, there is a huge increase (more than ten times) in the estimated RMS delay spread. This observation shows that, referring to the LoS propagation, the multipath components at the airborne altitude of 0.37 km have longer delays, which could be due to the significant evaporation ducting effect. The evaporation duct results in multireflections that have longer propagation paths.

IV. Propagation Loss Modeling and Analysis

For the propagation loss prediction of the aeronautical service, International Telecommunications Union (ITU)-R P.528 [18] recommends some propagation loss curves for different antenna heights (from 15 m to 20 km) at a large variety of frequencies (from 125 MHz to 15.5 GHz). According to the curve at the C-band (5.1 GHz), median (50%) propagation conditions approximate those of free space for path distances of about 45 to 95 km (distances used in our experiment). It is noted that the propagation model used to generate the curves is based on a considerable amount of experimental data [18]. However, our observation from multipath statistics in Section III shows that multiple propagation paths exist in about 86% of the measured channel responses, which can be represented by a 2-ray multipath model. Therefore, in this section, we will examine the measured propagation loss for the air-to-ground channel over the sea surface with the predicted results by the free space loss (FSL) model and the 2-ray loss model.

A. Propagation Loss Models

For the radio-wave propagation in free space, the propagation loss can be predicted by the FSL model [17] as

$$L_{\mathrm{FSL}}(\mathrm{dB}) = -27.56 + 20\log_{10}(f) + 20\log_{10}(d) \tag{2}$$

where L_{FSL} is the FSL in decibels, f is the frequency in megahertz, and d is the propagation distance in meters.

When a reflected ray exists besides the LoS component, the propagation loss can be predicted by a 2-ray loss model. Since there is a near-grazing incidence (maximum grazing angle during our measurements is about 2.3° at the path distance of 45 km with a flight altitude of 1.83 km), the reflection coefficient for vertical polarization approaches -1. Therefore, the 2-ray loss model can be simplified as in [17]

$$L_{2-\mathrm{ray}}(\mathrm{dB}) = -10\log_{10}\left\{\left(\frac{\lambda}{4\pi d}\right)^2\left[2\sin\left(\frac{2\pi h_T h_R}{\lambda d}\right)\right]^2\right\} \tag{3}$$

where $L_{2-\mathrm{ray}}$ is the 2-ray propagation loss in decibels, λ is the wavelength in meters, and h_T and h_R are the heights of the transmitter and receiver in meters, respectively. In the following part, both the FSL model and the 2-ray model will be used to predict the path loss under ideal conditions for air-to-ground propagation over the sea surface.

Moreover, the widely used "$10n\log_{10}(d)$" formulation as in [1] and [2] is also used in this study to empirically determine the radio-wave attenuation rate in the propagation channel

$$L(d) = A + 10n\log_{10}(d) \tag{4}$$

where L is the propagation loss in decibels, A is a constant, and n is the path-loss exponent. The path-loss exponent n and parameter A can be extracted from the measured data using the least mean square (LMS) curve-fitting technique.

B. Analysis of Air-to-Ground Over-Sea Channels

The estimated propagation loss versus distance with LMS curve fitting is plotted in Fig. 2 against the predicted loss using the FSL model and the 2-ray model (ideal case with perfect reflection) for each flight profile, respectively. From Fig. 2, it can be observed that the FSL model is not an appropriate model for the prediction of the propagation loss over the sea surface for air-to-ground transmission as recommended by ITU-R P.528. The measured losses are lower than those predicted by the FSL model. The main reason is that the propagation curves in ITU-R P.528 are based on data mainly obtained for a continental temperate climate. However, measurement results obtained in a tropical ocean climate (our study) are significantly different from those used by the ITU-R model. Moreover, if there is an evaporation duct over the sea surface during the measurements, the radio-wave propagation can be enhanced as reported in [10] and [19]. An enhancement larger than 10 dB was observed at 5.6 GHz in [19] 48% of the time along a 27.7-km over-sea path.

However, it is interesting to note from Fig. 2 that the measured results follow a similar trend to the predicted results from the 2-ray model. The destructive summation of the multipath signals arriving at the receiver results in the deep nulls in the estimated path loss. The results show that the air-to-ground channel over the sea surface can be approximately represented by a 2-ray model, as discussed in Section III. However, there are some measured deep nulls that are misaligned with the predicted deep nulls or are too weak. The misalignment is mainly due to the GPS data error, whereas the weak nulls are due to the wind-driven roughness of the sea surface. The median value of the average 5-min wind speed is found to be about 2.1 m/s, and the maximum wind speed is up to 3.8 m/s at the receiver during this measurement campaign. Sea-wind-driven roughened sea surface has been studied in [22] and found to reduce the specular sea-surface reflection in a ducting environment. The roughness of the sea surface can be intensified with the increase in sea-wind speed. However, due to the limitations of experimental condition in this study, the information on instantaneous sea-wind speed is lacking, and therefore, further investigations are required. Moreover, it is observed that the losses predicted by the 2-ray model are also higher than the measured losses. This is due to the existence of ducting effect. For the radio-wave propagation, ducts tend to form either when there is a temperature increase or when there is a water vapor concentration decrease, unusually rapidly with altitude. For the air-to-ground transmission over the sea surface, evaporation duct and elevated duct are the two main forms that could be experienced.

The possible evaporation/elevated duct over the sea surface and its transmission enhancement effect is investigated with the path-loss exponent n, which is estimated through the LMS curve fitting, as shown in Fig. 2, and is summarized in Table II for different airborne altitudes. From Table II, it is found that, for all the profiles, Channel 2 has a lower path-loss exponent n, compared with Channel 1. Since all other conditions are kept the same for both channels during the

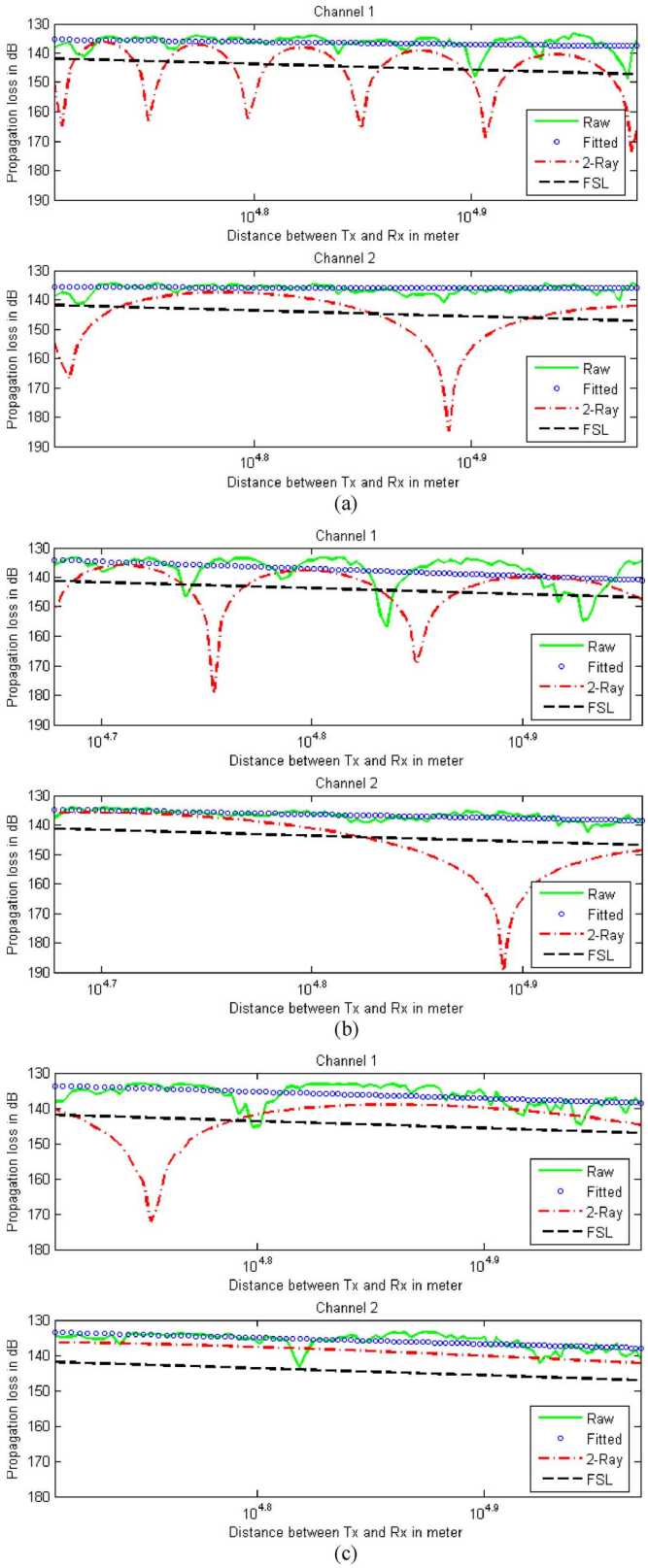

Fig. 2. Propagation loss versus distance at different altitudes with predicted loss from FSL and 2-ray models. (a) Results at an airborne altitude of 1.83 km (for the LMS line, $8.22\log_{10}(d) + 96.7$ at Channel 1 and $1.43\log_{10}(d) + 129$ at Channel 2). (b) Results at an airborne altitude of 0.91 km (for the LMS line, $24.6\log_{10}(d) + 19$ at Channel 1 and $13.5\log_{10}(d) + 71.6$ at Channel 2). (c) Results at an airborne altitude of 0.37 km (for the LMS line, $18.8\log_{10}(d) + 45.1$ at Channel 1 and $17.3\log_{10}(d) + 52$ at Channel 2).

TABLE II
SUMMARY OF PATH-LOSS EXPONENT AT DIFFERENT ALTITUDES

Antenna height	1.83 km	0.91 km	0.37 km
7.65 m @ Channel 1	0.82	2.46	1.88
2.10 m @ Channel 2	0.14	1.35	1.73

measurements, the lower path-loss exponent n for Channel 2 compared with that for Channel 1 is due to the difference in antenna height. It is noted that the antenna height at the receiver for Channe1 2 is about 2.10 m, and for Channel 1, it is about 7.65 m. The lower path-loss exponent n at Channel 2 with lower antenna height shows that the enhancement of transmission (lower path-loss exponent n, i.e., lower attenuation rate) is likely due to an evaporation duct over the sea surface, as discussed in [10] and [19] for the over-water radio-wave propagation. The evaporation duct exists over the ocean almost all of the time [20], because it is a result of the rapid decrease in vapor pressure from a saturation condition at the sea surface to an ambient vapor pressure at levels several meters above the sea surface. This decrease in vapor pressure generally results in a decrease in modified refractivity and, thus, a ducting layer adjacent to the sea surface. This ducting effect is obvious for the propagation channel with lower receiver height since there is a higher probability for the lower antenna to be located within the evaporation duct that is above the sea surface.

Moreover, it is found that the path-loss exponent n for the airborne altitude at 1.83 km is much smaller than those at 0.91 and 0.37 km. Since all other conditions are kept almost the same, the lower path-loss exponent n is due to the difference in the altitude of the airborne platform. It is known that, as the altitude of the airborne platform increases, the status of the troposphere such as humidity, pressure, and temperature along the propagation path changes. In addition to the evaporation duct that forms just above the sea surface (less than 40 m high from the modified refraction profile reported in [20]), other atmospheric ducts such as an elevated duct could start to affect the radio-wave propagation. Different from the evaporation duct, the ground base of an elevated duct is above the earth surface. Statistics derived from 20-year (1977–1996) radiosonde observations in ITU-R P.453 [23] indicates that, in our measurement region, the probability of yearly occurrence of elevated duct is more than 10% of the time and the average yearly elevated duct height is more than 1 km. On-site radiosonde data were also collected near the receiver location in this study. Although the measured radiosonde data have poor vertical resolution, it indicates the existence of an elevated duct with a height of about 0.9 to 1 km, which is close to the value obtained from ITU-R P.453 [23].

Comparing the three airborne altitudes for the air-to-ground propagation, it can be concluded that there is a higher probability for the signal coupling into the elevated duct at an airborne altitude of 1.83 km. This is consistent with the estimated path-loss exponent n. A lower path-loss exponent n (less than 1) is found for the flight profile at 1.83 km due to the enhancement of propagation from the elevated duct, compared with the propagation at the other two flight profiles (0.91 and 0.37 km).

V. CONCLUSION

This paper has reported on the experimental characterization and modeling of the air-to-ground channel over the sea surface at the C-band with low airborne altitudes. Results have shown that multipath propagation exists in the air-to-ground channel. Of the measured channel impulse responses, about 95% (86%) of the measured channel responses can be represented by the 3-ray (2-ray) multipath model. When the altitude of the airborne platform decreases, there is a higher probability for the appearance of multipath components.

The measured propagation loss has been compared with the predicted loss by the FSL and 2-ray models. Results have suggested that the measured losses follow a similar trend to those predicted by the 2-ray model. However, both the FSL and 2-ray models are found to overestimate the propagation loss. This is likely due to the propagation enhancements from evaporation and elevated ducts. The path-loss exponent n is then used to study the possible ducting effect on the propagation path. It is found that both the evaporation duct and the elevated duct can influence radio-wave propagation over the sea surface at the C-band. When the propagation path includes the evaporation and elevated ducts, the path-loss exponent n is found to decrease. However, the evaporation duct mainly affects the radio-wave propagation near the surface, and as the altitude of the airborne platform increases, the elevated duct will significantly contribute.

ACKNOWLEDGMENT

The authors would like to thank the anonymous reviewers and the associate editor for their constructive comments and suggestions for this paper.

REFERENCES

[1] D. W. Matolak, "Wireless channel characterization in the 5 GHz microwave landing system extension band for airport surface areas," Nat. Aeronat. Space Admin., Washington, DC, Final Project Rep., NASA CR-2007-214456, May 2007.

[2] D. W. Matolak, I. Sen, and W. Xiong, "The 5-GHz airport surface area channel—Part I: Measurement and modeling results for large airports," *IEEE Trans. Veh. Technol.*, vol. 57, no. 4, pp. 2014–2026, Jul. 2008.

[3] I. Sen and D. W. Matolak, "The 5-GHz airport surface area channel—Part II: Measurement and modeling results for small airports," *IEEE Trans. Veh. Technol.*, vol. 57, no. 4, pp. 2027–2035, Jul. 2008.

[4] H. D. Tu, S. Shimamoto, and J. Kitaori, "A proposal of a wide band for air traffic control communications," in *Proc. IEEE Wirel. Commun. Netw. Conf.*, Las Vegas, NV, Mar./Apr. 2008, pp. 1950–1955.

[5] Y. S. Meng and Y. H. Lee, "Investigations of foliage effect on modern wireless communication systems: A review," *Prog. Electromagn. Res.*, vol. 105, pp. 313–332, 2010.

[6] M. Rice, R. Dye, and K. Welling, "Narrowband channel model for aeronautical telemetry," *IEEE Trans. Aerosp. Electron. Syst.*, vol. 36, no. 4, pp. 1371–1376, Oct. 2000.

[7] M. Rice, A. Davis, and C. Bettweiser, "Wideband channel model for aeronautical telemetry," *IEEE Trans. Aerosp. Electron. Syst.*, vol. 40, no. 1, pp. 57–69, Jan. 2004.

[8] E. Haas, "Aeronautical channel modeling," *IEEE Trans. Veh. Technol.*, vol. 51, no. 2, pp. 254–264, Mar. 2002.

[9] Q. Lei and M. Rice, "Multipath channel model for over-water aeronautical telemetry," *IEEE Trans. Aerosp. Electron. Syst.*, vol. 45, no. 2, pp. 735–742, Apr. 2009.

[10] H. V. Hitney and L. R. Hitney, "Frequency diversity effects of evaporation duct propagation," *IEEE Trans. Antennas Propag.*, vol. 38, no. 10, pp. 1694–1700, Oct. 1990.

[11] Y. S. Meng, Y. H. Lee, and Y. H. Heng, "Channel characterization and modeling in C band for a small airport," in *Proc. 11th URSI Comm. F Symp. Radio Wave Propag. Remote Sens.*, Rio de Janeiro, Brazil, Oct./Nov. 2007, pp. 113–117.

[12] Y. H. Lee, Y. S. Meng, and Y. H. Heng, "Experimental characterizations of an air to land channel over sea surface in C band," in *Proc. XXIXth URSI Gen. Assem.*, Chicago, IL, Aug. 2008.

[13] Y. S. Meng and Y. H. Lee, "Practical wideband channel sounding system for air-to-ground measurements at C band," in *Proc. IEEE Int. Instrum. Meas. Technol. Conf.*, Singapore, May 2009, pp. 771–775.

[14] M. A. Jensen, M. D. Rice, and A. L. Anderson, "Aeronautical telemetry using multiple-antenna transmitters," *IEEE Trans. Aerosp. Electron. Syst.*, vol. 43, no. 1, pp. 262–272, Jan. 2007.

[15] J. Kivinen, T. O. Korhonen, P. Aikio, R. Gruber, P. Vainikainen, and S. G. Haggman, "Wideband radio channel measurement system at 2 GHz," *IEEE Trans. Instrum. Meas.*, vol. 48, no. 1, pp. 39–44, Feb. 1999.

[16] Y. S. Meng and Y. H. Lee, "Multipath characterization and fade mitigation of air-to-ground propagation channel over tropical sea surface at C band," in *Proc. IEEE APS Int. Symp. Antennas Propag.*, Toronto, ON, Canada, Jul. 2010, pp. 1–4.

[17] J. D. Parsons, *The Mobile Radio Propagation Channel*, 2nd ed. New York: Wiley, 2000.

[18] *Propagation Curves for Aeronautical Mobile and Radionavigation Services Using the VHF, UHF and SHF Bands*, ITU-R P.528-2, Int. Telecommun. Union, Jan. 1986.

[19] H. J. M. Heemskerk and R. B. Boekema, "The influence of evaporation duct on the propagation of electromagnetic waves low above the sea surface at 3–94 GHz," in *Proc. 8th Int. Conf. Antennas Propag.*, Edinburgh, U.K., Jan. 1993, pp. 348–351.

[20] J. G. Teti, Jr., "Wide-band airborne radar operating considerations for low-altitude surveillance in the presence of specular multipath," *IEEE Trans. Antennas Propag.*, vol. 48, no. 2, pp. 176–191, Feb. 2000.

[21] Y. S. Meng, Y. H. Lee, and B. C. Ng, "Investigation of rainfall effect on forested radio wave propagation," *IEEE Antennas Wireless Propag. Lett.*, vol. 7, pp. 159–162, 2008.

[22] X. Zhao and S. Huang, "Influence of sea surface roughness on the electromagnetic wave propagation in the duct environment," *Radioengineering*, vol. 19, no. 4, pp. 601–605, Dec. 2010.

[23] *The Radio Refractive Index: Its Formula and Refractivity Data*, ITU-R P.453-9, Int. Telecommun. Union, Jan. 2003.

Optimum Receiver Performance With Binary Phase-Shift Keying for Decode-and-Forward Relaying

M. D. Selvaraj, *Member, IEEE*,
Ranjan K. Mallik, *Senior Member, IEEE*, and Rupakshi Goel

***Abstract*—Cooperative diversity through decode-and-forward (DF) relaying is an effective method for improving the performance of mobile wireless systems. We consider here the performance of a cooperative diversity system in which the relay employs the DF protocol to transmit data from a source to a destination using binary phase-shift keying (BPSK). A flat Rayleigh fading environment with statistically independent links is assumed. The optimum receiver for this system is presented, and from the decision rule, the end-to-end symbol error probability (SEP) is derived. Numerical results on the SEP are obtained and compared with those for a suboptimum receiver, which does not need the channel state information of the source-to-relay link.**

***Index Terms*—Binary phase-shift keying (BPSK), decode-and-forward (DF) protocol, optimum receiver, Rayleigh fading, symbol error probability (SEP).**

I. INTRODUCTION

Transmitted signals from mobile units to a base station suffer from fading, meaning that rapid variations in the signal strength occur with respect to time. An effective and well-known technique for mitigating

Manuscript received December 11, 2009; revised April 19, 2010, August 30, 2010, and December 20, 2010; accepted February 4, 2011. Date of publication March 14, 2011; date of current version May 16, 2011. This work was supported in part by International Development Research Centre Research Grant RP02253. This paper was presented in part at the National Conference on Communications, Guwahati, India, January 16–18, 2009. The review of this paper was coordinated by Prof. Y. Gong.

M. D. Selvaraj is with the Department of Electronics and Electrical Communication Engineering, Indian Institute of Technology–Kharagpur, Kharagpur 721 302, India (e-mail: selvarajmd@yahoo.com).

R. K. Mallik is with the Department of Electrical Engineering, Indian Institute of Technology–Delhi, New Delhi 110 016, India (e-mail: rkmallik@ee.iitd.ernet.in).

R. Goel is with McKinsey & Company Inc., Gurgaon 122 001, India (e-mail: rupakshi@gmail.com).

Digital Object Identifier 10.1109/TVT.2011.2126611